Research Article

Journal of Molecular Recognition

Received: 9 August 2007, Revised: 13 November 2007, Accepted: 19 November 2007, Published online in Wiley InterScience: 2008

(www.interscience.wiley.com) DOI:10.1002/jmr.869

Probing the interaction between p53 and the bacterial protein azurin by single molecule force spectroscopy

Monia Taranta[a], Anna Rita Bizzarri[a]* and Salvatore Cannistraro[a]

p53 is a human tumour suppressor which regulates multiple cellular processes, including cell growth, genomic stability and cell death. Recent works have demonstrated the bacterial redox protein azurin to enter cancer cells and induce apoptosis through p53 stabilization, resulting in a tumour growth regression. Azurin has been shown to bind p53 although many details of the complex formed by these two proteins are still poorly characterized. Here, we get insight into the kinetics of this complex formation, by exploring the interaction between p53 and azurin in their environment by single molecule force spectroscopy. To this aim, azurin has been linked to the atomic force microscope tip, whereas p53 has been immobilized onto a gold substrate. Therefore, by performing force-distance cycles we have detected specific recognition events between p53 and azurin, displaying unbinding forces of around 70 pN for an applied loading rate of 3 nN s^{-1}. The specificity of these events has been assessed by the significant reduction of their frequency observed after blocking the p53 sample by an azurin solution. Moreover, by measuring the rupture force as a function of the loading rate we have determined the dissociation rate constant of this complex to be $\sim$0.1 s^{-1}. Our findings are here discussed in connection with results obtained in bulk experiments, with the aim of clarifying some molecular details of the p53-azurin complex that may help designing new anticancer strategy. Copyright © 2008 John Wiley & Sons, Ltd.

Keywords: p53; azurin; force spectroscopy; molecular interaction; cancer; AFM

INTRODUCTION

p53 is a transcription factor well known to have a key role in protecting cells against cancer (Levine, 1997; Vogelstein *et al*., 2000). This tumour suppressor is not pivotal for normal cell cycle progression, but turns out to be crucial under certain circumstances. p53, in fact, is kept at low levels in the cell by several factors that make it inactive or unstable and subject to degradation; but in response to various types of stress, such as DNA damage and hyperproliferative signals, it is rapidly activated and its intracellular levels are increased. Its activation can result either in cellular growth arrest and DNA repair or, eventually, in apoptosis, ensuring in this way the elimination of potentially cancerous cells (Levine, 1997). Activation of p53 is deeply related to its stabilization. In tumour cells that retain wild-type p53, often genes of factors responsible for its stabilization are found mutated (Ashcroft and Vousden, 1999). The identification of molecules that can restore the normal function of some mutated p53, or stabilize the wild-type, may thus pave the way for developing new targeted anticancer therapies.

Many reports show evidence of cancer regression mediated by bacteria, even if very little is known about the mechanism and the factors involved (Coley, 1991; Hunter *et al*., 2001). It has been demonstrated that some pathogens can replicate at tumour sites leading to cancer growth inhibition, but the side effects associated to the injection of live cells limit their use in cancer treatment. The employment of single proteins responsible for such phenomenon, conveniently engineered, may help surpassing this problem.

Recently, it has been reported that azurin, an electron transfer copper-containing protein from the bacterium *Pseudomonas aeruginosa*, can enter some mammalian cancer cells and induce apoptosis through p53-related pathway (Yamada *et al*., 2004). In the cells, azurin forms a complex with p53 and somehow stabilizes it and raises, with a positive feedback loop, its intracellular levels (Yamada *et al*., 2002a, 2002b; Goto *et al*., 2003). Once stabilized, p53 can carry out its tumour suppressor function, driving the cell to apoptosis. The effectiveness of this bacterial protein in cancer regression has been proven *in vivo*. Cancerous mice treated with azurin, in fact, have displayed a significant reduction of the tumour volume in comparison with the untreated ones (Yamada *et al*., 2004). Azurin capability of inducing apoptosis in tumour cells by p53 stabilization makes this protein suitable for being employed as anticancer agent.

Azurin (16 kDa) is a small globular metalloprotein, endowed with redox activity, involved in the bacterial denitrification process (Nar *et al*., 1991a; Solomon *et al*., 1992; Webb and Loppnow, 1999). This protein is well characterized and has been extensively studied by our group to explore its biophysical properties and its interactions with the redox partner cytochrome

* *Biophysics and Nanoscience Centre, CNISM, Facoltà di Scienze, Università della Tuscia, Largo dell'Università, 01100 Viterbo, Italy.*
E-mail: bizzarri@unitus.it

a *M. Taranta, R. Bizzarri, S. Cannistraro*
Biophysics and Nanoscience Centre, CNISM, Facoltà di Scienze, Università della Tuscia, Largo dell'Università, 01100 Viterbo, Italy

c551 (Paciaroni *et al.*, 1999; Bizzarri *et al.*, 2005; Bonanni *et al.*, 2005; Andolfi *et al.*, 2006).

p53 (53 kDa) is a protein made up of 393 residues, arranged into four functional regions: the N-terminal transactivation and the DNA binding domains, the tetramerization and the C-terminal regulatory domains, displaying large unstructured regions (Bell *et al.*, 2002; Dawson *et al.*, 2003). To date, the crystal structure of the full-length p53 has not been resolved, probably owing to the unfolded regions that make hard the crystallization process. Even the structure of the p53-azurin complex has not been determined. The regions of the two proteins involved in their interaction have been investigated by different approaches. Glycerol-gradient centrifugation experiments, followed by pull-down assays, show azurin to bind the N-terminal and the middle portion (amino acids 1–295) of p53 (Punj *et al.*, 2003). Docking simulations performed in our laboratory confirm the DNA-binding domain as an extremely probable binding region for azurin (De Grandis *et al.*, 2007). From calorimetric experiments, the N-terminal region of p53 has been identified as a binding site for the bacterial protein, and the dissociation constant (K_D) of the complex has been estimated (Apiyo and Wittung-Stafshede, 2005). About azurin, the region interacting with p53 has been identified by site-direct mutagenesis experiments, revealing the amino acids Met-44 and Met-64, located in a hydrophobic patch of the protein, critical for complex formation (Yamada *et al.*, 2002a).

The studies carried out until now in bulk provide some evidence on the formation of a complex between p53 and azurin but its structure and thermodynamics are described only to a small extent. However, these aspects should be fully characterized before the challenge of using azurin in cancer treatment can be faced.

In this paper, we try to get a deeper understanding on the kinetics of the p53-azurin complex, by probing the specific binding between these two proteins at the single molecule level, by means of the atomic force spectroscopy.

Atomic force microscopy (AFM) has been demonstrated to be a powerful tool for imaging biological samples in their physiological medium, resolving single molecules and without significantly perturbing their structure (Engel and Muller, 2000). Moreover, the AFM capability to feel the effect of forces in the order of picoNewton enables to measure the low forces of interactions that establish between molecules, by force spectroscopy experiments in physiological medium (Florin *et al.*, 1994; Lee *et al.*, 1994; Moy *et al.*, 1994). These experiments require the tethering of the two interacting partners, one to the AFM tip, and the other one to a stiff support. The strength of the protein–protein interaction is probed by performing force-distance cycles, in which the functionalized tip is approached to the sample allowing for the proteins to interact, and subsequently pulled back inducing their dissociation.

Here, p53 has been immobilized on a gold substrate, while azurin has been tethered to the AFM tip. Recognition events between p53 and azurin have been demonstrated to be specific by the remarkable reduction of unbinding frequency observed after blocking the p53 sample by a free azurin solution. The kinetics parameters determined from the force-distance cycles and the unbinding force detected indicate a significant stability of the complex here investigated. These findings represent a breakthrough in the understanding of the molecular details concerning the complex between p53 and azurin, which may be useful in developing antitumoural treatments, based on p53 stabilization.

MATERIALS AND METHODS

Tip functionalization

Azurin was purchased from Sigma-Aldrich (St. Louis, MO) and used without further purification, after dissolving in PBS 50 mM buffer pH 7. The Si_3N_4 cantilevers (Veeco Instruments, Santa Barbara, CA) were contact microlevers with backside gold coating and an oxide-sharpened tip. Probes were first cleaned in three changes of chloroform and then treated with amine groups by overnight incubation with ethanolamine-HCl dissolved in dimethylsulfoxide (DMSO). Next morning cantilevers were washed three times with DMSO, two times with ethanol and then dried with nitrogen. Then they were immersed in a solution of N-Succinimidyl-S-acetylthiopropionate (SATP) 2 mM in 10% DMSO and 90% 50 mM PBS buffer pH 7, for 2 h at room temperature. Subsequently, the cantilevers were immersed in a solution of 0.5 M hydroxylamine, 25 mM EDTA and 50 mM DTT in 50 mM PBS pH 7 for 20′. Tips were then rinsed with Milli-Q water, dried with nitrogen and immersed in 200 μl of 40 μM azurin in 50 mM PBS pH 7 for 2 h. After that, tips were gently washed and stored in buffer at 4°C.

Samples preparation

p53 (GST-p53 1.23 μM in 50 mM Tris-Acetate, pH 7.5, 1 mM EDTA, 20% Glycerol) was purchased from Millegen (Labège, France) and used without further purification. GST used to perform control experiments was kindly provided by Dr Ada Sacchi (IRE-Rome). The substrates consist of vacuum-evaporated thin gold films (thickness 250 nm) on borosilicate glass (Arrandee, Dr Dirk Schroer, Werther, Germany). These gold substrates were flame-annealed to obtain Au(111) terraces, and then immersed for 3.5 h in chloroform containing 0.2 mM $SHCH_2CH_2$-poly(ethylene glycol)-OCH_2CH_2COOH (PEG) (molecular weight 458.56; Sigma-Aldrich). The modified substrates were rinsed with chloroform and dried with nitrogen. The exposed carboxyl groups were then converted to amine-reactive NHS-esters according to the Pierce procedure. To this aim the gold modified surface were incubated with ~100 μl of a buffer (GST-p53 buffer) solution containing 0.2 mM EDC (Sigma-Aldrich) and 0.2 mM sulfo-NHS (Sigma-Aldrich) for 1 h at room temperature and then rinsed with buffer. Fifty microlitres of GST-p53 1.23 μM (or GST 1.2 μM) were poured onto this amine-reactive surface and allowed to react overnight at 4°C. Next morning, samples were gently rinsed with buffer solution to remove any unbound protein.

AFM imaging and force spectroscopy

A Nanoscope IIIa/Multimode AFM (Digital Instruments, Santa Barbara, CA) was used to image samples and to perform force spectroscopy experiments. p53 proteins were imaged in milliQ water by Tapping Mode AFM, fixing the amplitude set point to the 95% of the free amplitude value. The cantilever nominal spring constant was 0.5 N m^{-1}. Contact Mode AFM imaging and scratching were performed under air using a cantilever with a nominal spring constant of 0.02 N m^{-1}. The applied force was varied from few nN for imaging, to hundreds of nN for scratching. The AFM was used in force calibration mode to record force-distance cycles in 50 mM PBS pH 7. To limit the force that the tip applied to the surface, as well as to minimize deviations between experiments, a relative trigger of 23–35 nm was used in all force–distance curves. In all experiments the ramp size was

Journal of Molecular Recognition

150 nm and the approach velocity was set, through the software actuating the piezo scan of our AFM Nanoscope IIIa, operating in open loop configuration, equal to 72 nm s^{-1}, whereas the pulling velocity was varied from 35 to 2100 nm s^{-1}. The encounter time was set to zero. The cantilevers used to perform force spectroscopy studies had nominal spring constants of 0.01–0.03 N m^{-1}. The real cantilever spring constant of the functionalized tips was then determined by thermal noise analysis (Hutter and Bechhoefer, 1993).

RESULTS AND DISCUSSION

To perform single molecule recognition studies azurin has been linked to the AFM tip, according to an immobilization strategy that has already been successfully used in our group (Bonanni *et al*., 2006). As explained in more details in the Materials and Methods Section, the tip has been functionalized with a heterobifunctional crosslinker that bears, on its free end, a sulfhydryl-group, suitable for reacting with cysteine residues of the protein. Indeed, azurin has two cysteine residues exposed to solvent (Cys-3 and Cys-26) and involved in a disulphide bridge, just opposite to the hydrophobic patch that is deemed to interact with p53 (Nar *et al*., 1991b). Therefore, this linkage method allows azurin to orient itself with the hydrophobic patch facing the beneath p53 and thus maximizing the interaction probability (Yamada *et al*., 2002a).

p53 used in these experiments is a fusion protein GST-p53 but, for simplicity, from here on we will refer to it just as p53. This protein has been immobilized on a gold surface by means of a flexible poly(ethylene glycol) (PEG) linker, which contains a sulfhydryl-group on one end and a carboxyl-group on the other. Once anchored to the gold substrate by means of its sulfhydryl-group, the carboxyl moiety is available to react with an accessible p53 lysine residue, forming an amidic bond. The immobilization of proteins by covalent bonds—that are about 10-fold stronger then protein–protein interactions—ensures that when the tip is retracted only the interaction bond formed between partners results to be broken. The described immobilization strategy leads up to a pattern illustrated in Figure 1.

Before proceeding with force spectroscopy experiments, the morphology of p53 proteins immobilized on the gold has been analysed by AFM imaging, using a bare tip. Characteristic AFM images of such a sample are shown in Figure 2. Figure 2A, recorded by Tapping Mode AFM in fluid, shows a dense and homogenous monolayer of p53 molecules, in which the single proteins are clearly discernible. To assess the presence of only one protein layer on gold, we have performed scratching Contact Mode experiments under air, by which we have estimated the thickness of the film, as shown in Figure 2B. We can see that the depth of the hole caused by the tip scratching is around 5.5 nm and this is consistent with the thickness of a single protein layer. p53 samples prepared following the described strategy demonstrated to be reproducible and imaged proteins did not display mobility during the scan, indicating the formation of stable bonds, as expected for covalent ones.

Force-distance cycles have been recorded by approaching the tip at the constant velocity of 72 nm s^{-1}, whereas the pulling velocity has been varied according to the selected nominal loading rate. In fact, the loading rate—that is the rate at which a force is applied to the complex in the direction favouring the dissociate state—is defined as the product of the cantilever spring constant (k) by the tip retraction velocity (v). In all cycles, the maximum contact force value has been limited to 0.7 nN to avoid damage to the proteins, while the encounter time was set to zero. In our experiments, we have found primarily three different types of force–distance curves, all of which are depicted in Figure 3.

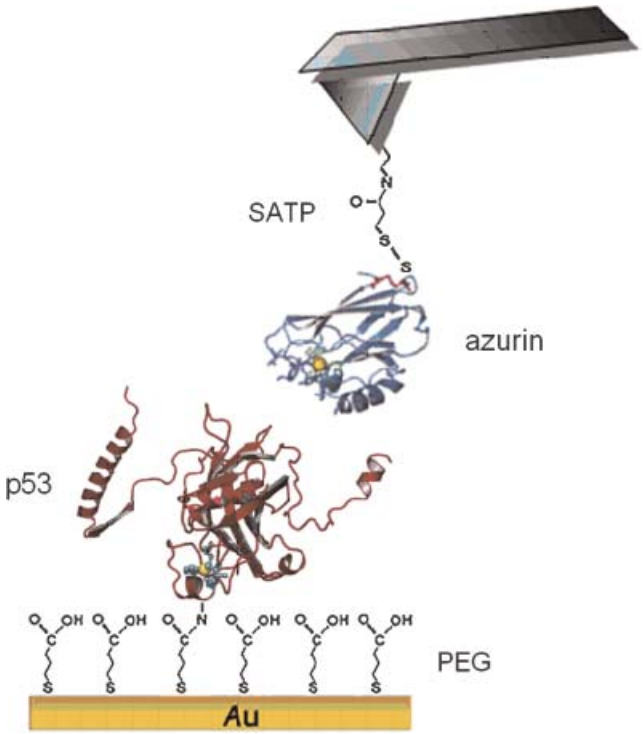

Figure 1. Immobilization strategy. Azurin is covalently linked to the AFM tip via the sulfhydryl-terminated spacer (SATP) that can bind one of the two accessible cysteine residues of the protein, represented in purple. p53 (approximate schematization, GST not represented) is immobilized on gold by means of a PEG crosslinker, which forms an S-Au bond with the gold, and an amidic bond with one of twenty-four accessible lysine residues of the protein.

Figure 3A is an example of force-curve displaying a specific unbinding event. The retraction curve, in fact, exhibits the characteristic stretching of the flexible polymer used to couple p53 proteins to the gold support, followed by the pull-off jump indicative of the specific unbinding (Willemsen *et al*., 1998; Heinz and Hoh, 1999). It has to be noted that such an event occurs far away from the point in which the tip leaves the monolayer surface and is characterized by a well-defined peak that originates and ends at the line of zero deflection. In the inset of Figure 3A, we show examples of force–distance curves with ambiguous pull-off jumps on the same curve. These curves have been discarded from our analysis to avoid the introduction of potentially 'false events' in the results. The second typology of observed force-curves is illustrated in Figure 3B. In this case, we can note that, during the retraction phase, the tip overstays in contact with the monolayer causing a hysteresis in the curve. This is due to an unspecific adhesion force, which depends only on the tip-sample interface, without involving the specific binding between the proteins and is characterized by the linear slope of the retrace (Willemsen *et al*., 1998; Heinz and Hoh, 1999). In the third type of force curve that we have found (not shown), the retraction curve faithfully follows the approach curve, suggesting the absence of any detectable unbinding event, both specific and

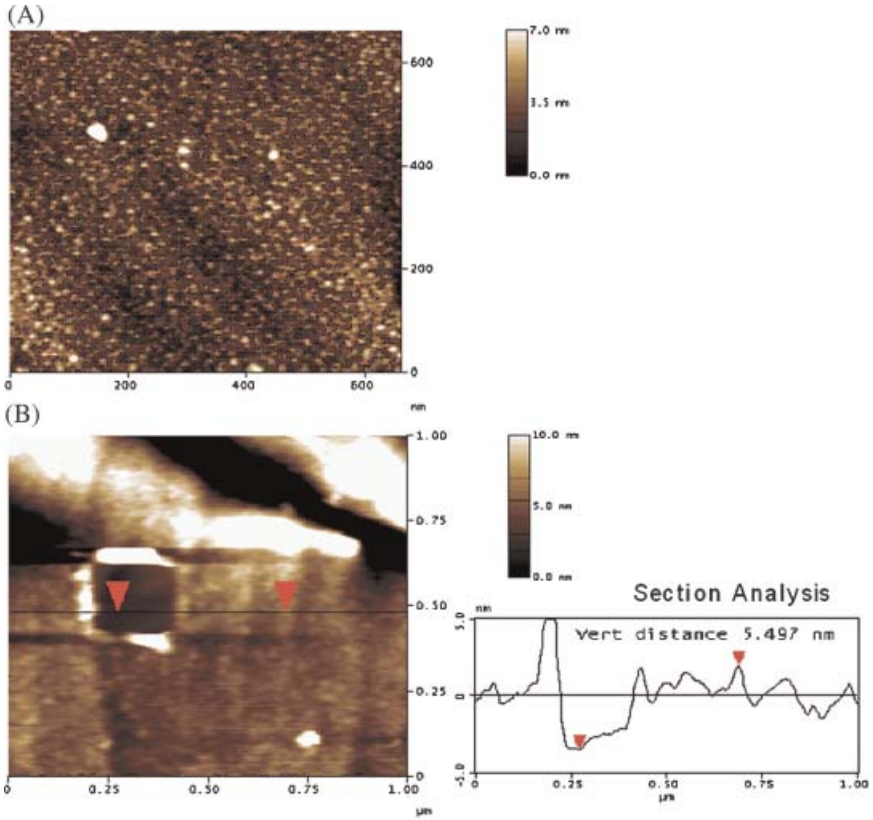

Figure 2. (A) Typical Tapping Mode AFM image of the p53 proteins immobilized on gold via PEG molecules, recorded under fluid environment. (B) Thickness of the layer assembled on the gold surface analysed by scratching the sample under air in Contact Mode.

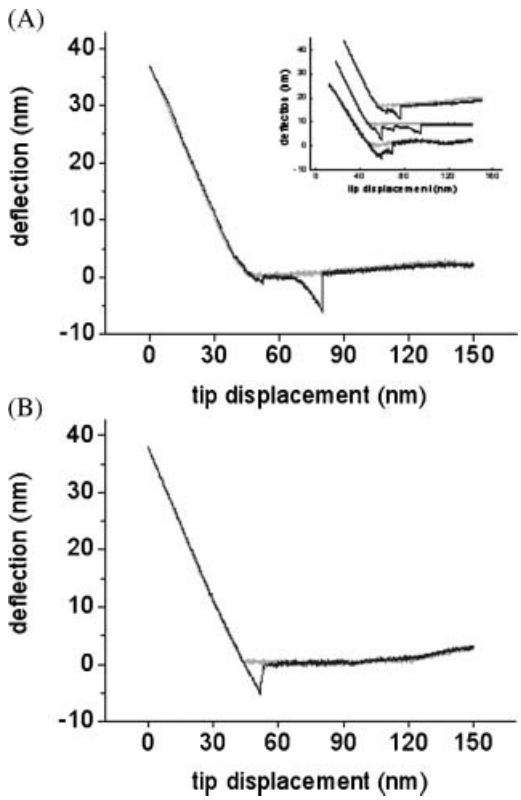

unspecific. Therefore, for the analysis of the interaction between p53 and azurin, we have specifically considered only the events similar to that illustrated in Figure 3A.

When we used a bare tip and a p53 sample to perform force-distance cycles, in the same experimental conditions earlier described, we observed curves displaying pull-off jumps with a frequency significantly lower than that observed with the azurin-charged tip (around 2.5%). Furthermore, experiments using an azurin functionalized tip and a gold substrate covered with GST proteins alone gave very few adhesion events, localized as a single population in a region of forces lower than 50 pN (data not shown).

Iterating of the 'approach-retract' process by means of the same tip has allowed us to record thousands of force curves over different regions of the sample, in which the probability of specific recognition events has been observed to be constant. The homogeneity of all these data confirmed that the molecules were tightly attached to their substrates (if they were pulled away, the unbinding frequency would have been reduced during the experiments). We have collected data by means of several functionalized tips and substrates and statistical distribution of

Figure 3. Typical force-distance curves recorded by an azurin functionalized tip over a p53 monolayer. (A) The retraction curve exhibiting a specific unbinding event, far away from the monolayer surface, anticipated by the stretching of the PEG linker. Inset: examples of ambiguous force-distance curves excluded from data analysis. (B) Example of curve displaying an unspecific event due to the adhesion force making the tip overstay in contact with the p53 sample. This event is characterized by the linear slope of the retrace extending beyond the contact line.

Journal of Molecular Recognition

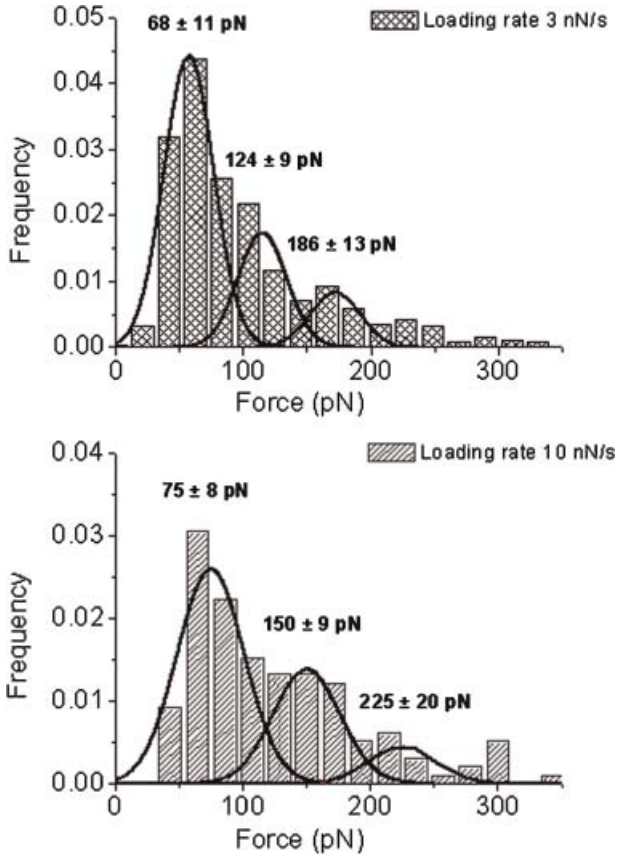

Figure 4. Force distributions of unbinding events recorded by applying loading rates of about 3 nN/s (top) 10 nN/s (bottom). The histograms were fitted to Gaussian functions to identify the most probable unbinding force values. This figure is available in colour online at www.interscience.wiley.com/journal/jmr

unbinding forces was found to be reproducible. Figure 4 displays typical force distributions obtained for unbinding events recorded by applying loading rates of about 3 and 10 nN s^{-1}. We note the presence of multiple peaks on each histogram; such behaviour becoming less pronounced lowering the loading rate. By fitting the histograms to Gaussian functions we found that the seconds and thirds peaks are centred at around twofold and threefold the value of the first ones, suggesting a quantization

Table 1. Unbinding force values obtained for various complexes by force spectroscopy experiments when a loading rate of 10 nN s^{-1} is applied

Complex	Force (pN)	References
Cadherin/cadherin	35 ± 16	Hinterdorfer *et al.* (2000)
Antilysozyme Fv fragment/lysozyme	55 ± 10	Berquand *et al.* (2005)
ExpG protein/DNA target sequence	75 ± 15	Bartels *et al.* (2003)
p53/azurin	75 ± 8	This work
Biotin/avidin	80 ± 15	De Paris *et al.* (2000)
Azurin/cytocrome c551	95 ± 15	Bonanni *et al.* (2005)
P-selectin/ligand	115 ± 40	Fritz *et al.* (1998)
Antifluorescein Fv fragment/fluorescein	160 ± 15	Schwesinger *et al.* (2000)

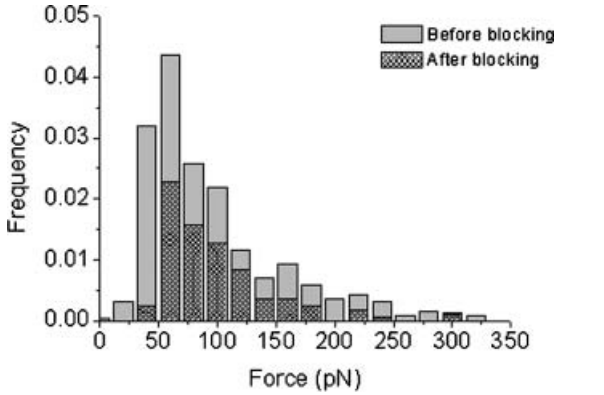

Figure 5. Comparison between unbinding force distributions of events recorded, at loading rate of about 3 nN/s, before and after blocking the p53 monolayer.

phenomenon (Florin *et al.*, 1994; Wong *et al.*, 1999). Accordingly, this finding suggests that the first peak represents the force of a single p53-azurin unbinding event that is about 68 pN at loading rate of 3 nN s^{-1} and 75 pN at loading rate of 10 nN s^{-1}.

It is commonly known that the unbinding force of a complex has not a unique value since it depends on the loading rate that the molecules feel when they are pulled apart. Accordingly, a dissociation force comparison between different complexes makes sense only if the compared values result from the application of the same loading rate. To get an idea about the range in which the p53-azurin complex is placed, in Table 1 we list some characteristic unbinding force values, for complexes studied in the literature, at a reference loading rate of 10 nN s^{-1}. 1. Even if it should be taken in mind that the declared loading rate could be somewhat different from the real ones, it is interesting to note that the complex here investigated falls within force values corresponding to other strong and highly specific biomolecular interactions.

From the analysis of the force-curves we have estimated the unbinding frequency on the total events to be about 19% (see Section 'Discussion' below). A similar binding probability has been noted also for azurin and cytochrome c551, which exhibits an 18% of specific interactions (Bonanni *et al.*, 2005). In that case, the relatively low binding frequency was hypothesized as due to the transient nature of the complex. It has to be considered that p53 are relatively big proteins (GST-p53 ~ 81 kDa) tightly packed on the gold substrate, as shown in Figure 2; this may result in some steric hindrance making the protein interaction less

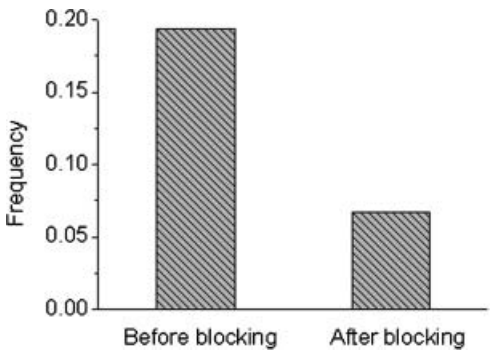

Figure 6. Unbinding force dependence on the applied loading rate. Force statistical errors are given by standard deviation. The line is obtained by fitting the experimental data by the Bell-Evans model.

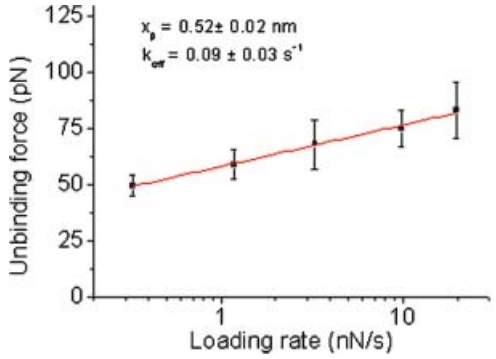

Figure 7. Unbinding frequencies observed before and after blocking the p53 monolayer by a free azurin solution. Each bar represents the unbinding frequency derived from 1000 force-distance curves. This figure is available in colour online at www.interscience.wiley.com/journal/jmr

favourable. Moreover, the presence of 24 lysine residues available to react with the linker may determine somewhat different orientations of p53 on the gold, some of which could display unfavourable geometry for the complex formation. Due to the occurrence of 19% binding, it could be argued that around five lysine residues might give rise to protein orientations suitable for positive binding events. All these factors certainly contribute to make relatively low the unbinding frequency (Figure 5).

To assess the specificity of recognition events, control experiments have been performed by recording force–distance curves after blocking the p53 monolayer by a 20 μM free azurin solution. Under these conditions, thousands of force-curves have been acquired over different sites of the sample and the unbinding force of the observed events has been measured. In Figure 6, the unbinding force distributions of events recorded before and after blocking the p53 monolayer are compared. We can note that in blocking experiments the occurrence of the events is reduced, while the shape of the forces distribution does not change, suggesting that the little activity observed in these conditions is of the same nature of that recorded before blocking. From a more detailed analysis of the pull-off jumps we have registered, upon blocking, a decrease of the specific events from the 19% to 7% (Figure 7), which is equivalent to a 63% reduction of the total recognition frequency recorded before blocking. The ability of an azurin solution to reduce the frequency of the observed interactions, without changing their intensity, strongly corroborates their specificity. The 7% of unbinding events is in agreement with other experiments that exhibit, even in effective blocking conditions, a residual binding activity (Hinterdorfer *et al*., 1996; De Paris *et al*., 2000; Bonanni *et al*., 2005, 2006).

Let us consider in more detail the dissociation kinetics of p53-azurin complex. In force spectroscopy experiments the rupture of the interaction bond takes place under the influence of an external force that drives the system away from the equilibrium, causing its escape from the bound state across the activation barrier. If the external force is applied slowly to the complex, it will have more chances to reach the transition state, so that the unbinding event will occur at lower forces. Therefore, we have explored the energy landscape of the complex between p53 and azurin, by measuring the unbinding force variation as a function of the loading rate. About thousand force curves have been recorded for every loading rate, and the corresponding most probable unbinding force has been assessed from the Gaussian fit of the histogram distributions. As earlier mentioned, we observed the presence of multiple peaks in the histograms, which presumably arise from one, two and three interactions, simultaneously broken. Recently, some authors have deeply analysed the multiple interactions of molecular complexes, investigating their force dependence on the applied loading rate (Sulchek *et al*., 2005; Odorico *et al*., 2007). Accordingly, it would be interesting to analyse our data along this line. However, in our case, occurrence of discernable multiple events is less frequent as long as the loading rate is reduced. Therefore, such an analysis cannot be applied in the present case. For this reason, to get insight into the energy landscape of the p53-azurin, we have restricted the analysis to the first peak of each distribution. When we fitted the force data as a function of the loading rate on the half logarithmic scale we have observed a roughly linear increase of the force values as shown in Figure 7. Several studies demonstrate a linear dependence of unbinding force on the logarithm of the applied loading rate, which can be justified in the context of the Bell–Evans model (Bell, 1978; Evans and Ritchie, 1997). This model, in fact, describes the unbinding process under the influence of an external force, allowing for evaluating some kinetics parameters of the complex under investigation. In particular, when a force is applied in the direction of the unbound state, the dissociation rate constant ($k_{off}(F)$) increases exponentially with the applied force

$$k_{off}(F) = k_{off} \cdot \exp[F\, x_\beta / k_B T] \quad (1)$$

where k_{off} is the dissociation rate constant in absence of the external force, x_β is the length scale of the energy barrier that is the distance that the ligand has to be moved to change from the bound to the transition state, k_B is the Boltzmann's constant and T the absolute temperature. Assuming that the applied force F increases linearly with a constant rate r ($F = r \cdot t$), the most probable unbinding force F' is then given by

$$F' = k_B T / x_\beta \cdot \ln[r\, x_\beta / k_{off} \cdot k_B T] \quad (2)$$

Therefore, by measuring the rupture force F' as a function of the loading rate r it is possible to determine the dissociation rate constant of the complex at zero force and the length scale of the energy barrier, and to assess the shape on the energy landscape. By plotting F versus $\ln(r)$, in fact, the x_β value can be obtained from the slope, whereas the k_{off} from the intercept.

We have performed these experiments by varying the tip retraction velocity from 35 nm s^{-1} to 2.1 μm s^{-1}. Then, the loading rate has been calculated by replacing the nominal cantilever spring constant with the effective one (k_{eff}). In fact, molecules, as proteins and linkers, tied to an AFM tip, make the cantilever spring constant change, so that it becomes necessary an estimation of the effective spring constant (k_{eff}) to determine the loading rate. We have evaluated the k_{eff} by measuring the linear part of the retraction curve preceding the unbinding event (De Paris *et al*., 2000; Yuan *et al*., 2000). For more reliability, we estimated this constant also according to a strategy recently adopted (Odorico *et al*., 2007), which takes into account the spring constant of the molecules tied to the AFM tip, that is, however, related to the slope of the unbinding event. The values obtained by these two methods are in agreement within the error.

The plot in Figure 7 highlights, at least in the loading rates range here taken into account, the presence of a single regime with a uniform slope, from which we have estimated x_β to be 0.52 ± 0.02 nm and k_{off} to be 0.09 ± 0.03 s^{-1}.

Journal of Molecular Recognition

Table 2. Dissociation rate constant values obtained for various complexes by force spectroscopy experiments

Complex	k_{off} (s^{-1})	References
Biotin/avidin	$\sim 10^{-6}$	Yuan *et al.* (2000)
Antigen/antibody	$\sim 10^{-4}$–10^{-1}	Schwesinger *et al.* (2000)
p53/azurin	$\sim 10^{-1}$	This work
Cadherin/cadherin	~ 1.8	Baumgartner *et al.* (2000)
Azurin/cytocrome c551	~ 6–14	Bonanni *et al.* (2005, 2006)
DNA/sfiI	~ 38	Krasnoslobodtsev *et al.* (2007)

Both the x_β and k_{off} extrapolated from our data analysis are in the range of values found also for other complexes (Baumgartner *et al.*, 2000; Yuan *et al.*, 2000). The off-rate is in the range of those obtained for ligand-receptor and antigen-antibody pairs, which exhibit $k_{off} \sim 10^{-4}$–$10^{-1}\,s^{-1}$ as can be inferred from Table 2 where, for greater clarity, k_{off} values for different complexes are listed. The lifetime the p53-azurin complex at zero force (τ_0) has been also estimated to be $\sim$11 s, according to $\tau_0 = 1/k_{off}$ (Bell, 1978).

Besides determining the dissociation rate constant value for this complex, we have also got an estimation of its association rate constant (k_{on}). To this aim, we have varied the interaction time between the proteins, observing an exponentially increasing of the unbinding frequency with the contact time, until the reaching of a maximum value. From these data we have assessed the time required for the half-maximal binding probability, $t_{0.5}$, to be about 0.06 s. Moreover, we have estimated that the radius r_{eff} of the half-sphere, which describes the effective volume for proteins binding (V_{eff}) (Hinterdorfer *et al.*, 1996), was about 4 nm. These observations led us to calculate the association rate constant $k_{on} = N_A V_{eff}/t_{0.5} = 1.5 \cdot 10^4\,M^{-1} \cdot s^{-1}$. The assessment of both the dissociation and association rate constants have allowed us to determine that the dissociation constant ($K_D = k_{off}/k_{on}$) for the complex between p53 and azurin is about $6 \cdot 10^{-6}$ M. This value positions the p53-azurin complex in an 'affinity region' located between the transient azurin-cytochrome c551 complex ($K_D \sim 10^{-4}$–10^{-6} M) (Wilson *et al.*, 1975), and the antigen-antibody pairs ($K_D \sim 10^{-7}$–10^{-11} M). These findings indicate that the complex between p53 and azurin is significantly stable. Experiments performed in bulk reveal a strong affinity between these two proteins, but with a lower K_D value (about 33 nM) in one case (Apiyo and Wittung-Stafshede, 2005), and with a K_D comparable with our result in another case (Strambini *et al.*, personal communication). Our results point out a substantial affinity of azurin for p53, that is, however, lower than that found for p53 and its best-known inhibitor MDM2 (Chène, 2004), which binds the N-terminal region of the protein (Chi *et al.*, 2005). We can speculate that azurin may interact with a different region of p53, competing with other molecules that down regulate p53, or sterically protecting target sites for degradation. For example, if azurin would interact with the DNA binding domain of p53 as described by Punj *et al.* (2003) and De Grandis *et al.* (2007), it could either prevent the binding of other degradation proteins or sterically protect some crucial ubiquitination sites (Chan *et al.*, 2006). Alternatively, azurin may bind to the N-terminal region as recently proposed by Apiyo and Wittung-Stafshede (2005), likely with a direct competition with MDM2.

CONCLUSIONS

The specific interaction between p53 and azurin has been here investigated, directly in their physiological environment, for the first time at the level of single molecule. By exploring the energy landscape of this complex dissociation we have estimated important parameters of the p53-azurin complex that were not available until now. The specificity of the biorecognition has been proven by control blocking experiments, in which we observed a drastic reduction of the unbinding events, displaying the same pattern of force distributions. The unbinding force estimated for p53-azurin complex is in the range of forces found for other specific biological interactions. But more importantly, the k_{off} value of about $0.1\,s^{-1}$ obtained from these experiments, the corresponding K_D estimated and the lifetime of 11 s, indicate that the complex between p53 and azurin is substantially stable. These aspects suggest that azurin can promote the p53 activation through strategies operating with mechanisms whose full clarification could lead to establish pharmacological strategies restoring the p53 function.

Acknowledgements

We thank Dr Beatrice Bonanni for experimental advises, Dr Valentina De Grandis for generating Figure 1 and Dr Ada Sacchi for kindly providing the GST sample. Thanks are due to the 'Dipartimento di Scienza dei Materiali dell'Università di Lecce' for financial support to one of the authors (M. T.). The work was partially supported by an Innesco-CNISM project 2005 and by two PRIN-MIUR 2006 projects (n. 2006028219 and 2006027587).

REFERENCES

Andolfi L, Bizzarri AR, Cannistraro S. 2006. Assembling of Redox Proteins on Au(111) Surfaces: a Scanning Probe Microscopy Investigation for Application in Bio-Nanodevices. *Thin Solid Films* **515**: 212–219.

Apiyo D, Wittung-Stafshede P. 2005. Unique complex between bacterial azurin and tumor-suppressor protein p53. *Biochem. Biophys. Res. Commun.* **332**: 965–968.

Ashcroft M, Vousden KH. 1999. Regulation of p53 stability. *Oncogene* **18**: 7637–7643.

Bartels FW, Baugmarth B, Anselmetti D, Ros R, Becker A. 2003. Specific binding of the regulatory protein ExpG to promoter regions of the galactoglucan biosynthesis gene cluster of *Sinorhizobium meliloti*—a combined molecular biology and force spectroscopy investigation. *J. Struct. Biol.* **143**: 145–152.

Baumgartner W, Hinterdorfer P, Ness W, Raab A, Vestweber D, Schindler H, Drenckhahn D. 2000. Cadherin interaction probed by atomic force microscopy. *Proc. Natl. Acad. Sci. U S A* **97**: 4005–4010.

Bell GI. 1978. Models for the specific adhesion of cells to cells. *Science* **200**: 618–627.
Bell S, Klein C, Muller L, Hansen S, Buchner J. 2002. p53 contains large unstructured regions in its native state. *J. Mol. Biol.* **322**: 917–927.
Berquand A, Xia N, Castner DG, Clare BH, Abbott NL, Dupres V, Adriaensen Y, Dufrene YF. 2005. Antigen bindingforces of single antilysozyme Fv fragments explored by atomic force microscopy. *Langmuir* **21**: 5517–5523.
Bizzarri AR, Andolfi L, Stchakovsky M, Cannistraro S. 2005. AFM, STM and Ellipsometry Characterization of a monolayer of azurin molecules self-assembled on a gold surface in air. *Online J. Nanotech.* **1**: 1–11.
Bonanni B, Kamruzzahan ASM, Bizzarri AR, Rankl C, Gruber HJ, Hinterdorfer P, Cannistraro S. 2005. Single molecule recognition between cytochrome c551 and gold-immobilized azurin by force spectroscopy. *Biophys. J.* **89**: 2783–2791.
Bonanni B, Bizzarri AR, Cannistraro S. 2006. Optimized biorecognition of cytochrome c551 and azurin immobilized on thiol-terminated monolayers assembled on Au(111) substrates. *J. Phys. Chem. B* **110**: 14574–14580.
Chan WM, Mak MC, Fung TK, Lau A, Siu WY, Poon RY. 2006. Ubiquitination of p53 at multiple sites in the DNA-binding domain. *Mol. Cancer Res.* **1**: 15–25.
Chène P. 2004. Inhibition of the p53-MDM2 Interaction: targeting a Protein-Protein Interface. *Mol. Cancer Res.* **2**: 20–28.
Chi S-W, Lee S-H, Kim D-H, Ahn M-J, Kim J-S, Woo J-Y, Torizawa T, Kainosho M, Han K-H. 2005. Structural Details on mdm2-p53 Interaction. *J. Biol. Chem.* **46**: 38795–38802.
Coley WB. 1991. The treatment of malignant tumors by repeated inoculations of erysipelas with a report of ten original cases: 1983 classical article. *Clin. Orthop. Relat. Res.* **262**: 3–11.
Dawson R, Muller L, Dehner A, Klein C, Kessler H, Buchner J. 2003. The N-terminal domain of p53 is natively unfolded. *J. Mol. Biol.* **332**: 1131–1141.
De Grandis V, Bizzarri AR, Cannistraro S. 2007. *J. Mol. Recogn.* **20**: 215–226.
De Paris R, Strunz T, Oroszlan K, Guntherold H-J, Hegner M. 2000. Force spectroscopy and dynamics of the biotin-avidin bond studied by scanning force microscopy. *Single Mol.* **1–4**: 285–290.
Engel A, Muller D. 2000. Observing single molecules at work with the atomic force microscope. *Nat. Struct. Biol.* **7**: 715–718.
Evans E, Ritchie K. 1997. Dynamic strength of molecular adhesion bonds. *Biophys. J.* **72**: 1541–1555.
Florin EL, Moy VT, Gaub HE. 1994. Adhesion forces between individual ligand-receptor pairs. *Science* **264**: 415–417.
Fritz JA, Katopodis G, Kolbinger F, Anselmetti D. 1998. Force mediated kinetics of single P selectin/ligand complexes observed by atomic force microscopy. *Proc. Natl. Acad. Sci. U S A* **95**: 12283–12288.
Goto M, Yamada T, Kimbara K, Horner J, Newcomb M, Das Gupta TK, Chakrabarty AM. 2003. Induction of apoptosis in macrophages by *Pseudomonas aeruginosa* azurin: tumour-suppressor protein p53 and reactive oxygen species, but not redox activity, as critical elements in cytotoxicity. *Mol. Microbiol.* **47**: 549–559.
Heinz WF, Hoh JH. 1999. Spatially resolved force spectroscopy of biological surfaces using the atomic force microscope. *Trends Biotechnol.* **17**: 143–150.
Hinterdorfer P, Baumgartner W, Gruber HJ, Schilcher K, Schindler H. 1996. Detection and localization of individual antibody-antigen recognition events by atomic force microscopy. *Proc. Natl. Acad. Sci. U S A* **93**: 3477–3481.
Hinterdorfer P, Kienberger F, Raab A, Gruber HJ, Baumgartner W, Kada G, Riener C, Wielert-Badt S, Borken C, Schindler H. 2000. Poly(Ethylene Glycol): an ideal spacer for molecular recognition force microscopy/spectroscopy. *Single Mol.* **1–2**: 99–103.
Hunter CA, Yu D, Gee M, Ngo CV, Sevignani C, Goldschmidt M, Golovkina TV, Evans S, Lee WF, Thomas-Tikhonenko A. 2001. Cutting edge: systemic inhibition of angiogenesis underlies resistance to tumor during acute toxoplasmosis. *J. Immunol.* **166**: 5878–5881.
Hutter JL, Bechhoefer J. 1993. Calibration of atomic force microscope tips. *Rev. Sci. Instrum.* **64**: 1868–1873.
Krasnoslobodtsev AV, Shlyakhtenko LS, Lyubchenko YL. 2007. Probing interactions within the synaptic DNA-Sfil complex by AFM force spectroscopy. *J. Mol. Biol.* **365**: 1407–1416.
Lee GU, Kidwell DA, Colton RJ. 1994. Sensing discrete streptavidin-biotin interactions with atomic force microscopy. *Langmuir* **10**: 354–357.
Levine AJ. 1997. p53, the cellular gatekeeper for growth and division. *Cell* **88**: 323–331.
Moy VT, Florin EL, Gaub HE. 1994. Intermolecular forces and energies between ligands and receptors. *Science* **266**: 257–259.
Nar H, Messerschmidt A, Huber R, van de Kamp M, Canters GW. 1991a. Crystal structure analysis of oxidized *Pseudomonas aeruginosa* azurin at pH 5.5 and pH 9.0. A pH-induced conformational transition involves a peptide bond flip. *J. Mol. Biol.* **221**: 765–772.
Nar H, Messerschmidt A, Huber R, van de Kamp M, Canters GW. 1991b. X-ray crystal structure of the two site-specific mutants His35Gln and His35Leu of azurin from *Pseudomonas aeruginosa*. *J. Mol. Biol.* **218**: 427–447.
Odorico M, Teulon JM, Bessou T, Vidaud C, Bellanger L, Chen SW, Quéméneur E, Parot P, Pellequer JL. 2007. Energy landscape of chelated uranyl: antibody interactions by dynamic force spectroscopy. *Biophys. J.* **93**: 645–654.
Paciaroni A, Stroppolo ME, Arcangeli C, Bizzarri AR, Desideri A, Cannistraro S. 1999. Incoherent neutron scattering of copper azurin: a comparison with molecular dynamics simulation results. *Eur. Biophys. J.* **28**: 447–456.
Punj V, Das Gupta TK, Chakrabarty AM. 2003. Bacterial cupredoxin azurin and its interactions with the tumor suppressor protein p53. *Biochem. Biophys. Res. Commun.* **312**: 109–114.
Schwesinger F, Ros R, Strunz T, Anselmetti D, Guntherodt H-J, Honegger A, Jermutus L, Tiefenauer L, Pluckthun A. 2000. Unbinding forces of single antibody-antigen complexes correlate with their thermal dissociation rates. *Proc. Natl. Acad. Sci. U S A* **97**: 9972–9977.
Solomon EI, Baldwin MJ, Lowery MD. 1992. Electronic structures of active sites in copper proteins: contributions to reactivity. *Chem. Rev.* **92**: 521–542.
Sulchek TA, Friddle RW, Langry K, Lau EY, Albrecht H, Ratto TV, DeNardo SJ, Colvin ME, Noy A. 2005. Dynamic force spectroscopy of parallel individual Mucin1-antibody bonds. *Proc. Natl. Acad. Sci. U S A* **102**: 16638–16643.
Vogelstein B, Lane DP, Levine AJ. 2000. Surfing the p53 network. *Nature* **408**: 307–310.
Webb MA, Loppnow GR. 1999. A structural basis for long-range coupling in azurins from resonance Raman spectroscopy. *J. Phys. Chem. A* **103**: 6283–6287.
Willemsen OH, Snel MME Snel, van der Werf KO, de Grooth BG, Greve J, Hinterdorfer P, Gruber HJ, Schindler H, van Kooyk Y, Figdor CG. 1998. Simultaneous height and adhesion imaging of antibody-antigen interactions by atomic force microscopy. *Biophys. J.* **75**: 2220–2228.
Wilson MT, Greenwood C, Brunori M, Antonini E. 1975. Electron transfer between azurin and cytochrome c-551. *Biochem. J.* **145**: 449–457.
Wong J, Chilkoti A, Moy VT. 1999. Direct force measurements of the streptavidin-biotin interaction. *Biomol. Eng.* **16**: 45–55.
Yamada T, Goto M, Punj V, Zaborina O, Chen ML, Kimbara K, Majumdar D, Cunningham E, Das Gupta TK, Chakrabarty AM. 2002a. Bacterial redox protein azurin, tumor suppressor protein p53, and regression of cancer. *Proc. Natl. Acad. Sci. U S A* **99**: 14098–14103.
Yamada T, Goto M, Punj V, Zaborina, Kimbara K, Das Gupta TK, Chakrabarty AM. 2002b. The bacterial redox protein azurin induces apoptosis in J744 macrophages through complex formation and stabilization of the tumor suppressor protein p53. *Infect. Immun.* **70**: 7054–7062.
Yamada T, Hiraoka Y, Ikehata M, Kimbara K, Avner BS, Das Gupta TK, Chakrabarty AM. 2004. Apoptosis or growth arrest: modulation of tumor suppressor p53's specificity by bacterial redox protein azurin. *Proc. Natl. Acad. Sci. U S A* **101**: 4770–4775.
Yuan C, Chen A, Kolb P, Moy VT. 2000. Energy landscape of streptavidin-biotin complexes measured by atomic force microscopy. *Biochemistry* **39**: 10219–10223.